Trajectory Control for a Low-Lift Re-Entry Vehicle

Axel J. Roenneke*
University of Stuttgart, 70176 Stuttgart, Germany
and
Phillip J. Cornwell†
Rose-Hulman Institute of Technology, Terre Haute, Indiana 47803

This paper presents re-entry trajectory control for a small re-entry vehicle by path following. A tracking controller restricts the vehicle to a multivariable reference trajectory defined by altitude, velocity, and flight-path angle. The controller design is based on several linear system models along a desired reference trajectory. A linear control law is designed to minimize a quadratic performance index at discrete points on the reference. Simulation results of spatial flights over a rotating Earth show that the designed controller effectively responds to entry condition offsets on several reference trajectories. Also, the controller is capable of tolerating changing vehicle parameters as well as atmospheric disturbances. The same controller gain functions are successfully applied to different reference trajectories.

Nomenclature

$A(t)$ = reduced-order plant matrix
$B(t)$ = reduced-order control matrix
C_D = drag coefficient
C_L = lift coefficient
D = drag acceleration, normalized by G_0
$F(t)$ = feedback gain matrix
G_0 = acceleration of gravity at sea level
g = acceleration of gravity, normalized by G_0
L = lift acceleration, normalized by G_0
m = mass of vehicle
n_G = aerodynamic load factor
$P(t_k)$ = solution of the algebraic Riccati equation
Q = diagonal weighting matrix
R_0 = radius of the Earth
r = distance from the Earth's center, normalized by R_0
S = reference area
t = flight time, normalized by $\sqrt{R_0/G_0}$
v = Earth-relative speed, normalized by $\sqrt{G_0R_0}$
$x(t)$ = state vector
γ = flight-path angle
$\delta x(t)$ = reduced-order state error vector
ϵ = lift-to-drag ratio, C_L/C_D
θ = geodetic longitude
ρ = atmospheric density
σ = bank angle
ϕ = geodetic latitude
ψ = heading angle
ω = Earth's angular velocity, normalized by $\sqrt{G_0/R_0}$

Introduction

FUTURE space projects, such as laboratories stationed in orbit, will only be attractive if transportation can be provided at low operational cost. Economic alternatives to the manned Space Shuttle are unmanned and reusable payload vehicles with a low lift-to-drag ratio. Their feasibility is currently being investigated in the United States and Europe.[1-4] A key issue is, if safe and accurate landing can be achieved despite the vehicles' limited aerodynamics, to avoid an expensive recovery and long turnaround periods. A simple and reliable control system must restrict the vehicles to a flight path inside the load limits subject to unexpected parameter variations. The control system must respond to off-nominal entry conditions and must be tolerant to aerodynamic uncertainties and atmospheric disturbances. Finally, the system must function autonomously without ground or pilot control.

In the past, re-entry guidance has been built on a combination of two different strategies[5,6]: path prediction, in which the controller computes a new trajectory in advance based on the actual flight conditions, and path following, in which the controller tries to reach a predetermined trajectory. Traditionally, reference trajectories are selected from the acceleration-velocity plane, since range can be expressed as the integral of drag over velocity. Thus, measuring velocity, a vehicle is guided to the desired final state by scheduling drag or vertical acceleration.

The Gemini[7] and the second entry phase Apollo[8] guidance laws track a stored lift-to-drag reference. In flight, the schedule is corrected based on the estimated downrange error, and acceleration and velocity feedback are used to eliminate tracking errors. The same principle is applied in the U.S. Space Shuttle entry guidance.[9,10] A drag vs velocity schedule inside the load corridor is selected and can be updated during entry to achieve the required downrange. A drag and velocity feedback law locally tracks this drag profile.

Self-reliant predictor methods have been suggested for the inertial upper stage vehicle[11] and NASP[12] as well as for low-lift capsules.[2,13] Based on current flight conditions, these systems use numerical fast-time integration of the future trajectory to determine the control input during re-entry. Eventually, this technique may be combined with optimization procedures[14,15] to select a desired input from performance criteria. However, with current technology standards, the computing hardware required for these programs is regarded as too bulky and complex to be feasible for a small payload vehicle.

In contrast to predictive methods, the concept described in this paper is based entirely on path following. Reference trajectories are prescribed for three states: altitude, velocity, and flight-path angle. Onboard satellite navigation is used to provide position and velocity updates. This concept requires a minimum of navigation and control hardware. In this ap-

proach, a feedback control system eliminates trajectory offsets resulting from entry condition dispersions, atmospheric disturbances, and aerodynamic uncertainties. Whether the reference path is obtained by a particular guidance law or an optimization procedure does not affect the control concept and is not a subject of this paper.

Multiple-state feedback is a feasible design approach. Current flight conditions can be obtained from satellite navigation in addition to conventional onboard inertial measurement units (IMUs). Receivers for the Navstar Global Positioning System (GPS) are available for spacecraft application with a total mass of 6 kg and the size of a car stereo.[16] They ascertain position and velocity at a sample rate of 200 Hz with an accuracy of ±30 m and ±0.3 m/s, respectively, even if the spacecraft is traveling at orbital speeds. Integrated systems, cross-filtering GPS and IMU information for higher accuracy, are under development and have been successfully used for autonomous approach and landing of aircraft.[17]

The controller design is based on several linear system models along a feasible trajectory. Feedback gain functions are computed by linear quadratic regulator optimization. This design approach has been presented in previous papers.[18,19] In this paper, the control system performance is investigated when it is responding to entry condition dispersions of several states. Simultaneously, the control system is submitted to aerodynamic and atmospheric variations. How one set of gain functions performs on reference trajectories that are different from the design trajectory is also evaluated.

Re-Entry Model and Test Vehicle

To demonstrate the trajectory control problem, we have chosen a specific mission and vehicle model. The translational motion of a rigid body over a rotating, spherical Earth is used as the nonlinear system model to simulate unpowered re-entry glide and the controller performance. The forces acting on the vehicle are gravity and the aerodynamic lift and drag. Wind is not considered.

The state of the vehicle is represented by standard Earth-fixed variables[20,21]:

$$x(t) = [r \; v \; \gamma \; \psi \; \theta \; \phi]^T \tag{1}$$

where v is the normalized velocity. Flight-path angle γ and heading angle ψ give the direction of the velocity vector. The control of the vehicle is represented by the velocity bank angle σ, which is formed by the lift vector and the local vertical plane. The dynamics of a roll maneuver are disregarded in this analysis.

In terms of these state and control variables, the dynamic system is given by

$$\dot{r} = v \sin \gamma \tag{2}$$

$$\dot{v} = -D - g \sin \gamma$$
$$+ \omega^2 r \cos \phi(\cos \phi \sin \gamma - \sin \phi \cos \gamma \sin \psi) \tag{3}$$

$$\dot{\gamma} = 1/v [L \cos \sigma - (g - v^2/r)\cos \gamma + 2\omega v \cos \phi \cos \psi$$
$$+ \omega^2 r \cos \phi (\cos \phi \cos \gamma + \sin \phi \sin \gamma \sin \psi)] \tag{4}$$

$$\dot{\psi} = \frac{1}{v} \left[L \frac{\sin \sigma}{\cos \gamma} - \frac{v^2}{r} \tan \phi \cos \gamma \cos \psi \right.$$
$$\left. - \omega^2 r \frac{\sin \phi \cos \phi \cos \psi}{\cos \gamma} + 2\omega v (\cos \phi \tan \gamma \sin \psi - \sin \phi) \right]$$
$$\tag{5}$$

$$\dot{\theta} = \frac{v \cos \gamma \cos \psi}{r \cos \phi} \tag{6}$$

$$\dot{\phi} = \frac{v \cos \gamma \sin \psi}{r} \tag{7}$$

The overdot indicates differentiation with respect to nondimensional time t. For the following simulation results, a Newtonian gravity law $g = 1/r^2$ is assumed.

Lift and drag accelerations L and D are related to the dimensional speed $V = v\sqrt{G_0 R_0}$ and the atmospheric density ρ by the following common definitions:

$$L = \frac{S}{2mG_0} C_L \rho V^2 \tag{8}$$

$$D = \frac{S}{2mG_0} C_D \rho V^2 \tag{9}$$

Both quantities are normalized by the acceleration of gravity at sea level.

The load factor n_G is defined as the magnitude of the aerodynamic acceleration:

$$n_G = \sqrt{L^2 + D^2} \tag{10}$$

Equations (8–10) show that n_G only depends on the altitude-velocity path of the vehicle's trajectory.

Vehicle data used in the following are taken from a European design study on a small re-entry module.[1] The vehicle has a sphere-cone configuration with a base diameter of 0.5 m and a height of 0.8 m. The total mass is estimated at 80 kg. To provide aerodynamic lift, one side of the cone is flattened, resulting in a constant supersonic lift-to-drag ratio of 0.52. The capsule's attitude can be changed by moving the center of gravity, for example, via a servo-controlled ballast mass. In the simulation, this capability is modeled as a variation of the velocity bank angle.

Trajectory Control Concept

Perturbation guidance combined with trajectory tracking is a well-known guidance method[5-8,22,23] and has also been considered for re-entry guidance of vehicles with moderate lift-to-drag ratio. In a recent tradeoff study on guidance for aeroassisted orbital transfer missions, this method ranked best with respect to performance and required onboard computing power.[4] It is the goal of current research to investigate whether such a concept is also effective in controlling the re-entry trajectory of a low-lifting vehicle.

This paper presents a tracking control law for the fast dynamics of the re-entry equations represented by altitude, velocity, and flight-path angle. Terminal control for the slow dynamics given by the position and heading angles can be achieved independently from the fast dynamics and is not addressed in the following.

The controller design is based on the trajectory error with respect to the three reference states. In this fashion, the trajectory control problem is cast into a multivariable tracking problem. For low-lifting vehicles, it can be shown that re-entry trajectories are slowly varying.[5,24] To track a reference, a linear regulator concept is sufficient. Measuring the state errors, the controller continuously adjusts the bank angle to correct the actual trajectory and to match the reference.

For the controller design, a reduced-order linear system is defined with respect to the trajectory error. Let the subscript R denote the reference state and control histories, respectively. For small deviations $\delta x = [r - r_R, \; v - v_R, \; \gamma - \gamma_R]^T$ and $\delta \sigma = \sigma - \sigma_R$, the state equations can be written in linear form as

$$\delta \dot{x} = A(t)\delta x + B(t)\delta \sigma \tag{11}$$

The reduced-order system matrix $A(t)$ and the reduced-order control matrix $B(t)$ are approximated at discrete times t_k by constant matrices $A(t_k)$ and $B(t_k)$, which are obtained numerically at the reference state. For our controller design, $A(t_k)$ and $B(t_k)$ are the corresponding Jacobian submatrices of the

state equations (2-7). This approximation is equivalent to assuming a stationary Earth.

Theoretically, a linear control law for a time-varying system must be based on $A(t)$ and $B(t)$ as functions of time. However, since these functions are slowly varying,[24] $A(t_k)$ and $B(t_k)$ can be treated as locally time invariant for the design. Thus, at each time t_k, a linear control law is suggested of the form

$$\delta\sigma = -F(t_k)\delta x \tag{12}$$

where the feedback gains $F(t_k)$ are constant. These gains are obtained by minimizing an infinite-horizon quadratic performance criterion

$$\lim_{t_f\to\infty}\int_0^{t_f}(q_1\delta r^2 + q_2\delta v^2 + q_3\delta\gamma^2 + q_\sigma\delta\sigma^2)\,\mathrm{d}t \tag{13}$$

with constant nonnegative weighting coefficients q_i on state and control errors. This problem is commonly referred to as linear quadratic regulator optimization.[25] Since the system is controllable, the feedback gains are given by

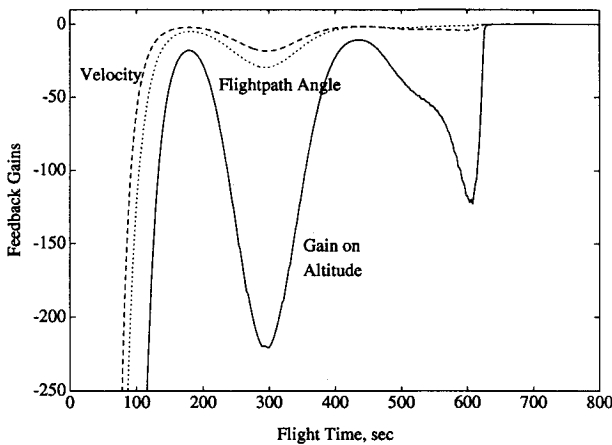$$F(t_k) = \frac{1}{q_\sigma}B^T(t_k)P(t_k) \tag{14}$$

Fig. 1 Feedback gains vs time. Data points are obtained by successive solution of the algebraic Riccati equation.
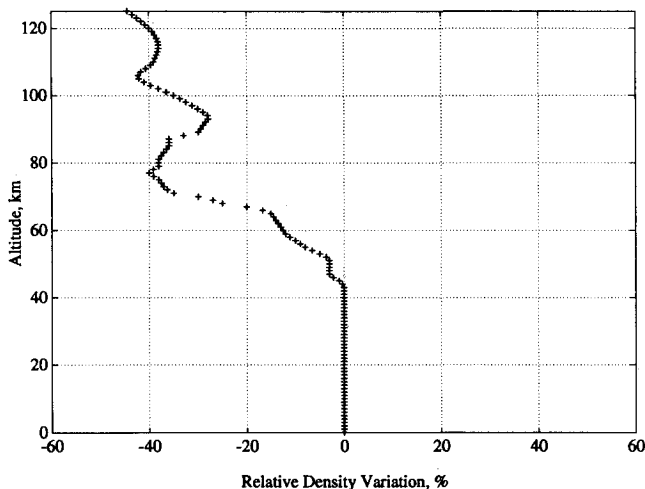

Fig. 2 North latitude atmospheric density data from Ref. 27. Altitude is plotted vs relative density variation from the U.S. Standard Atmosphere 1976.

Table 1 Nominal and off-nominal entry conditions for a payload re-entry vehicle; off-nominal entry conditions result from a 10% larger or smaller deorbit impulse

Impulse perturbation, %	+ 10	0	− 10
Altitude, km	120	120	120
Velocity, m/s	7422.5	7440.3	7458.3
Flight-path angle, deg	− 3.30	− 2.97	− 2.60

The constant matrix $P(t_k)$ is the solution of the algebraic Riccati equation

$$0 = Q - PB\frac{1}{q_\sigma}B^TP + PA + A^TP \tag{15}$$

where Q contains the weighting coefficients:

$$Q = \mathrm{diag}\,(q_1,\,q_2,\,q_3) = \mathrm{diag}\,(1,\,0.1,\,10) \tag{16}$$

The numerical values of q_i are chosen according to Bryson's rule.[23] Each term of the integrand in Eq. (13) contributes, on average, equally to the performance index. A typical gain schedule $F(t_k)$ calculated for the nominal reference trajectory and nominal conditions is shown in Fig. 1.

Error Sources

The re-entry mission is divided into three phases. At deorbit, the vehicle is jettisoned from a space station in a low-Earth orbit of 500-km altitude at a 28.5-deg inclination. The capsule goes into a Keplerian transfer orbit and reaches the detectable atmosphere at a 120-km altitude and a flight-path angle of − 2.8 deg. This is the interface to atmospheric re-entry. The capsule passes through the atmosphere on an aerodynamic glide, during which a feedback law controls the vehicle to a reference trajectory. The final approach phase begins when the vehicle is parachuted from an altitude of 5 km to the ground. Simulation results in the following show the atmospheric part of re-entry until parachute deployment.

To evaluate the controller performance, several model parameters are changed simultaneously to an off-nominal value. We have considered entry condition offsets of several states, atmospheric density disturbances, and a constant offset from the vehicle's nominal lift-to-drag ratio. Lastly, how one set of controller gains performs on different reference trajectories is investigated.

The transfer orbit is modeled as a Hohmann ellipse[22] with a fictitious perigee altitude of − 200 km. Deorbit is induced by a single impulse opposing the orbit velocity vector. To represent entry condition dispersions, the nominal deorbit impulse is offset by ± 10%. This perturbation is well within the expected retroboost error of 1%. The resulting entry conditions at a 120-km altitude are listed in Table 1.

For nominal flight conditions, atmosphere data are taken from the U.S. Standard Atmosphere 1976.[26] During the controller simulation, the atmospheric density is changed to data measured during Space Shuttle entry flights with north latitude.[27] This density profile is up to 50% lower than the U.S. Standard Atmosphere 1976 between 120- and 40-km altitudes (see Fig. 2).

To model design uncertainties, the nominal lift-to-drag ratio of 0.52 is varied by ± 4%. This value compares with experiences from the Apollo program.[28] During the controller simulation, the lift-to-drag ratio is changed to 0.50 or 0.54, respectively.

Controller Performance

For the following simulation results, reference trajectories are chosen with constant 30-, 45-, and 60-deg bank angles, respectively. At nominal entry and parameter conditions, the 45-deg trajectory is chosen as the design trajectory for the
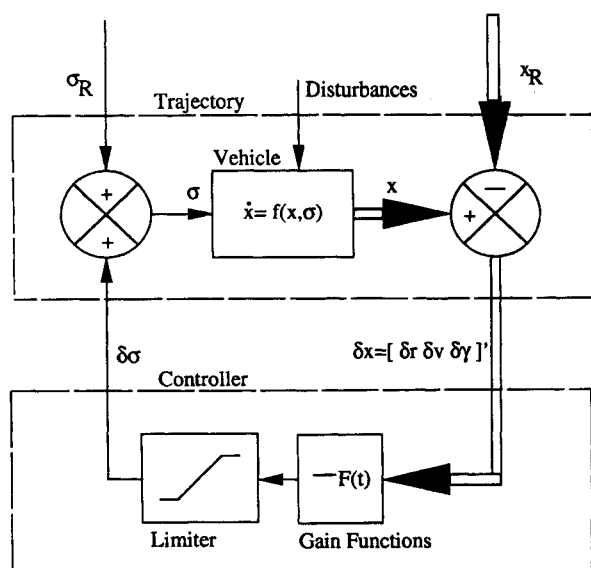
Fig. 3 Block diagram schematic of the simulated feedback system. The nonlinear equations of motion are contained in the vehicle block.
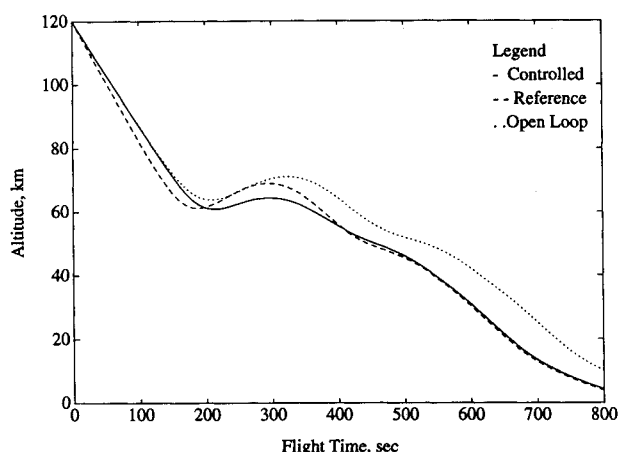
controller. Although this range of trajectories is chosen arbitrarily, it covers the vehicle's lifting capabilities[2] and agrees with the vehicle's design specifications.[1] With constant bank angles of 60 deg or lower, the capsule develops enough vertical lift so that the aerodynamic acceleration does not exceed the desired limit of 3 g. A bank angle of a constant 45 deg also provides maximum lateral reach.[21]

A block diagram schematic of the simulated control system is shown in Fig. 3. The reduced-order regulator receives feedback of the state errors in altitude, velocity, and flight-path angle. With these offsets, the controller computes the necessary change in bank angle. A saturation block limits the bank angle input to a range from 0 to 90 deg. Thus, neither heading reversals nor negative-lift maneuvers are permitted. The response of the system to a set of entry conditions is integrated numerically in the time domain using the system analysis program Simulink.[29]

Figures 4–6 show the time histories of altitude, velocity, and flight-path angle due to a 10% lower deorbit impulse. Simultaneously, the lift-to-drag ratio of the controlled vehicle is increased by 4% to 0.54. The controller smoothly counteracts the higher initial speed and also approaches the desired histories of altitude and flight-path angle. The controlled vehicle stays close to the desired trajectory after 400 s. The load factor

Fig. 4 Altitude time history of the feedback regulator system to entry conditions resulting from a 10% smaller deorbit impulse. Simultaneously, the vehicle's lift-to-drag ratio is increased by 4%. The reference trajectory (dashed line) and the open-loop time history (dotted line) are plotted for comparison.
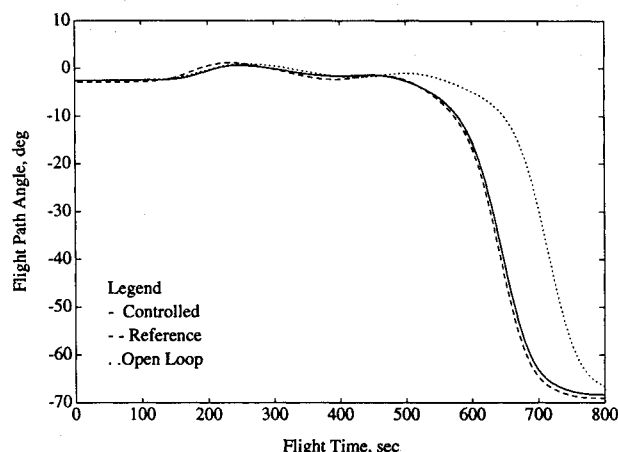

Fig. 6 Flight-path angle time history of the feedback regulator system to entry conditions resulting from a 10% smaller deorbit impulse. Simultaneously, the vehicle's lift-to-drag ratio is increased by 4%.

Fig. 5 Velocity time history of the feedback regulator system to entry conditions resulting from a 10% smaller deorbit impulse. Simultaneously, the vehicle's lift-to-drag ratio is increased by 4%.
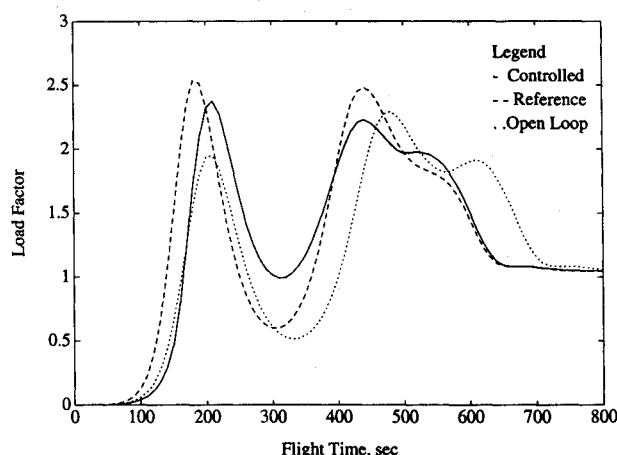

Fig. 7 Load factor time history of the feedback regulator system to entry conditions resulting from a 10% smaller deorbit impulse. Simultaneously, the vehicle's lift-to-drag ratio is increased by 4%.

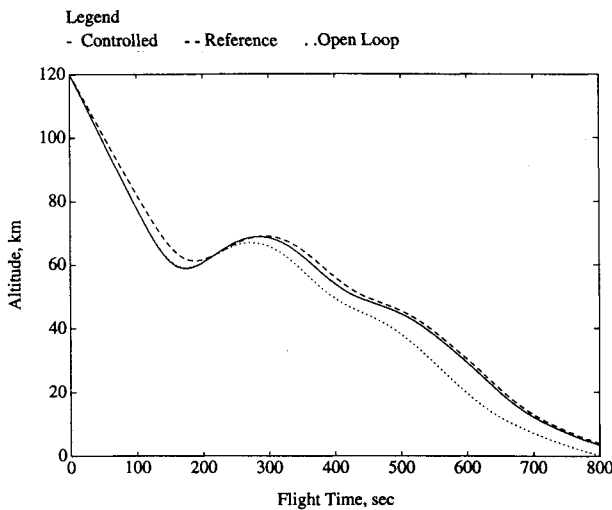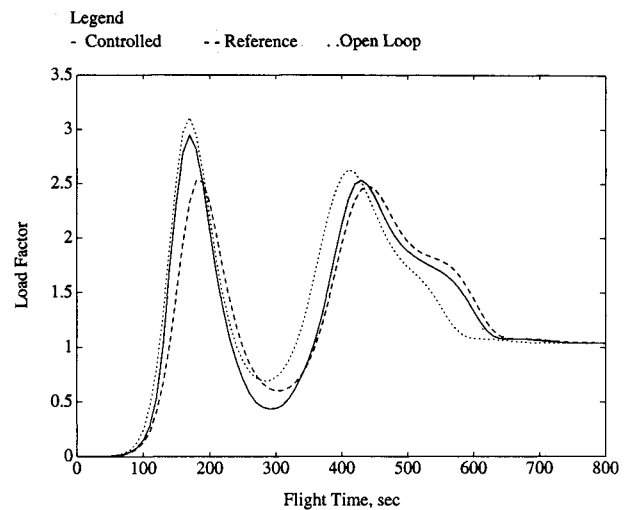Legend
- Controlled - - Reference . .Open Loop

Fig. 8 Altitude time history of the feedback regulator system to entry conditions resulting from a 10% larger deorbit impulse. Simultaneously, the vehicle's lift-to-drag ratio is decreased by 4%.

Legend
- Controlled - - Reference . .Open Loop

Fig. 11 Load factor time history of the feedback regulator system to entry conditions resulting from a 10% larger deorbit impulse. Simultaneously, the vehicle's lift-to-drag ratio is decreased by 4%.
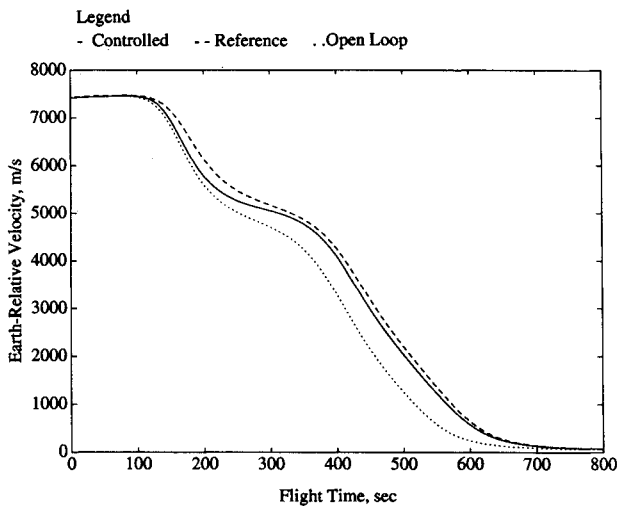
Legend
- Controlled - - Reference . .Open Loop

Fig. 9 Velocity time history of the feedback regulator system to entry conditions resulting from a 10% larger deorbit impulse. Simultaneously, the vehicle's lift-to-drag ratio is decreased by 4%.
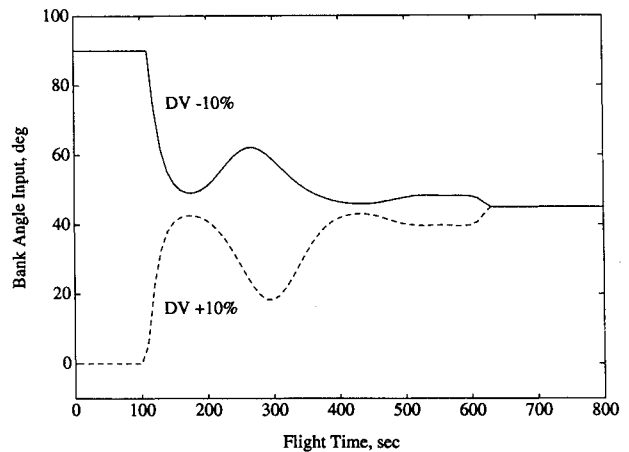
Fig. 12 Bank angle input time history as commanded by the controller for a 45-deg reference trajectory. Response of the feedback regulator system to entry conditions resulting from ±10% deorbit impulse perturbations.

Legend
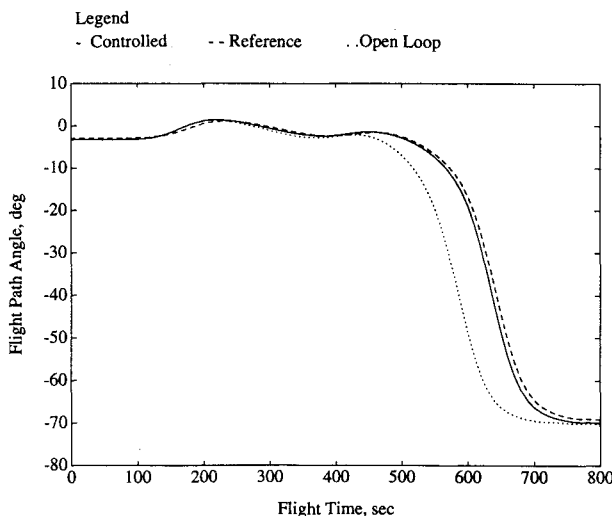- Controlled - - Reference . .Open Loop

Fig. 10 Flight-path angle time history of the feedback regulator system to entry conditions resulting from a 10% larger deorbit impulse. Simultaneously, the vehicle's lift-to-drag ratio is decreased by 4%.

experienced by the controlled vehicle (see Fig. 7) does not differ greatly from the values on the desired path.

A second case with opposite parameter offsets is presented in Figs. 8–10. The plots show the time histories of altitude, velocity, and flight-path angle due to a 10% higher deorbit impulse, resulting in a lower entry speed and a more shallow flight-path angle (see Table 1). At the same time, the lift-to-drag ratio of the controlled vehicle is decreased by 4% to 0.50. Again, the controller is able to counteract these offsets and guide the vehicle to the desired trajectory. The controlled vehicle's speed increases when compared with the uncontrolled time history and approaches the desired trajectory asymptotically. The altitude and flight-path angle histories approach the desired within satisfactory final error limits. The control action has lowered the load factor curve of the controlled vehicle (see Fig. 11), but the peak load on the controlled path exceeds the desired peak value.

The bank angle histories for the two previous cases are plotted in Fig. 12. It shows that the transients for opposite speed and angle offsets are mirror images. For both cases, the bank angle histories are smooth functions with one oscillation. The required roll rate is less than 1 deg/s. This result shows

that the presented control law is suitable for a vehicle with slow attitude dynamics.

Strictly speaking theoretically, one computed gain schedule is only valid for the particular reference trajectory for which it is designed. However, for practical applications, how a single set of gain functions performs on neighboring reference trajectories that are different from the design trajectory is of interest. The following test results show that the gain schedules designed for the 45-deg reference trajectory also do well on trajectories with constant 30- and 60-deg bank angles.

Figures 13, 14, and 17 show the time histories of altitude, velocity, and the bank angle input due to a 10% larger deorbit impulse on a 30-deg reference trajectory. The vehicle approaches the desired trajectory eventually, but slower and later than on the 45-deg reference (Figs. 8 and 9). On a 60-deg reference with a 10% smaller deorbit impulse (Figs. 15–17), the performance of the controller compares with the results from the 45-deg reference (Figs. 4 and 5).

These results demonstrate that the proposed state feedback law, which is designed for one particular reference trajectory, controls the vehicle to several reference trajectories. For practical applications, this implies that the number of gain sched-
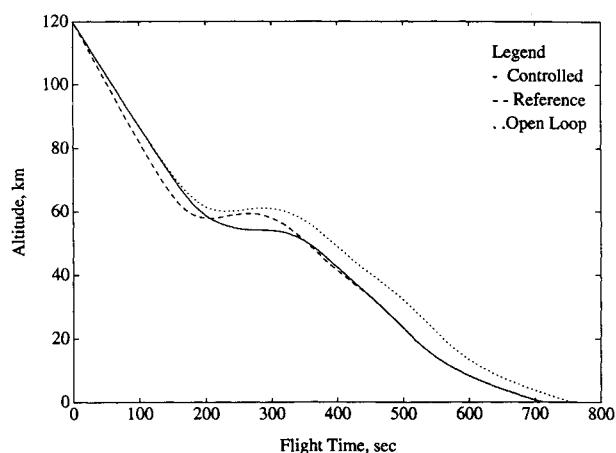

Fig. 15 Altitude time history of the feedback regulator sytem to entry conditions resulting from a 10% smaller deorbit impulse. The reference trajectory is computed with constant 60-deg bank angle, whereas the controller gains are designed for a 45-deg reference trajectory.
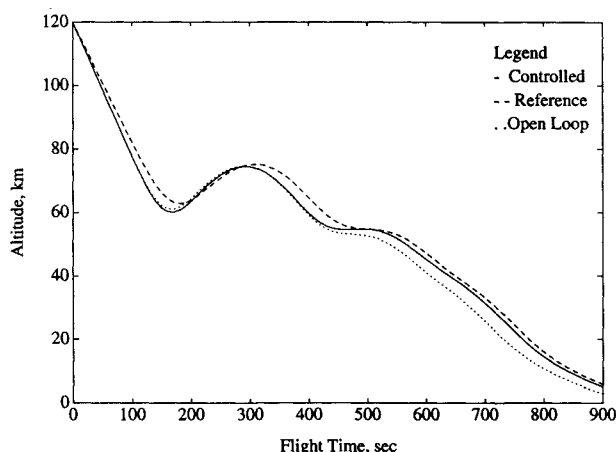

Fig. 13 Altitude time history of the feedback regulator system to entry conditions resulting from a 10% larger deorbit impulse. The reference trajectory is computed with constant 30-deg bank angle, whereas the controller gains are designed for a 45-deg reference trajectory.
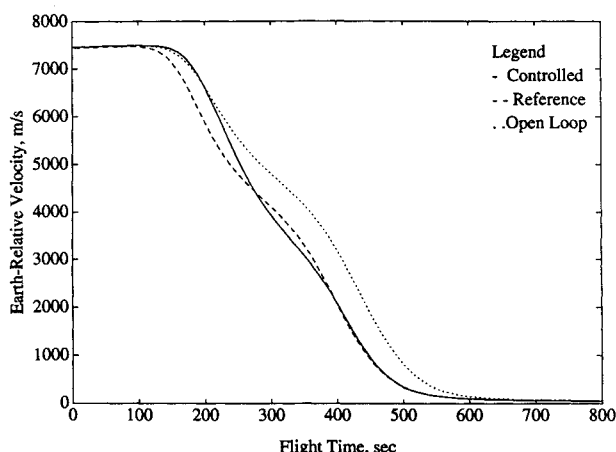

Fig. 16 Velocity time history of the feedback regulator system to entry conditions resulting from a 10% smaller deorbit impulse. The reference trajectory is computed with constant 60-deg bank angle, whereas the controller gains are designed for a 45-deg reference trajectory.
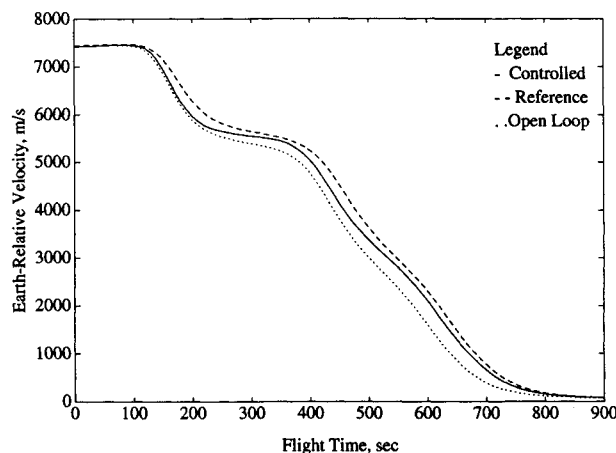

Fig. 14 Velocity time history of the feedback regulator system to entry conditions resulting from a 10% larger deorbit impulse. The reference trajectory is computed with constant 30-deg bank angle, whereas the controller gains are designed for a 45-deg reference trajectory.
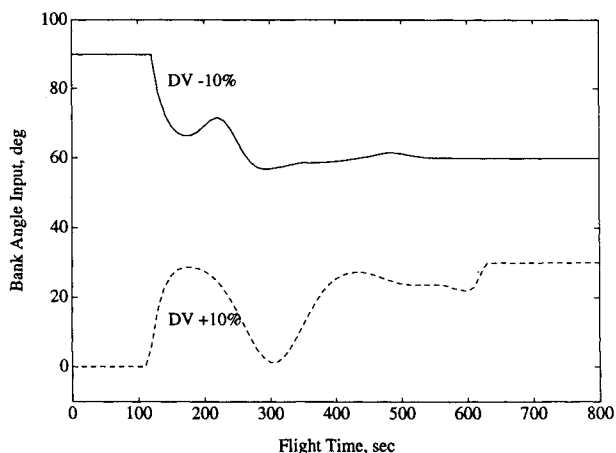

Fig. 17 Bank angle input time history as commanded by the controller for 30- and 60-deg reference trajectories. The system responds to 10% deorbit impulse perturbations. The controller gains are designed for a 45-deg reference trajectory.

ules stored aboard the spacecraft may be limited without sacrificing performance. This, combined with the simplicity of the design, also makes the described trajectory control system attractive for implementation in onboard prediction methods.

Summary and Conclusions

This paper presents re-entry trajectory control for a small re-entry vehicle by path following. A tracking controller restricts the vehicle to a multivariable reference trajectory defined by altitude, velocity, and flight-path angle. The controller design is based on a system model obtained by successively linearizing the equations of motion along a desired reference trajectory. The linear control law is designed to minimize a quadratic performance index at discrete points on the reference.

The results in this paper show that the proposed controller responds effectively to several parameter changes applied simultaneously: entry condition offsets resulting from deorbit impulse perturbations of $\pm 10\%$, changes in the lift-to-drag ratio of $\pm 4\%$, and atmospheric density variations of up to 50%. The commanded variation of the velocity bank angle is smooth and does not require roll rates of more than 1 deg/s. The presented results show that the performance of the controller is also satisfactory on reference trajectories that are different from the design trajectory.

We plan to apply the path control system presented here to advanced guidance laws, including terminal control. A path controller is used to improve the accuracy of the pursued trajectory and to reduce landing site dispersions.

Acknowledgments

References

[1]Aenishanslin, M. H., "Space Mail Feasibility Study," Société Nationale Industrielle Aérospatiale, Columbus Preparatory Programme Rept. COL-TN-AS-0050, Les Mureaux, France, Nov. 1986.

[2]Schöttle, U., Bregman, E. R., Hil, Hillesheimer, M., and Inatani, Y., "Conceptual Study of a Small Semiballistic Re-Entry Experiment Vehicle," 41st Congress of the International Astronautical Federation (Dresden Germany), IAF-90-163, Oct. 1990.

[3]Tong, D., "Payload Vehicle Aerodynamic Re-Entry Analysis," *Journal of Spacecraft and Rockets*, Vol. 29, No. 5, 1992, pp. 641-645.

[4]ACRI—Laboratoire d'Automatique de Nantes, "Guidance and Control for Moderate Lift/Drag Re-Entry," European Space and Technology Center, CR 9359-91-NL-JG, monitored by D. Paris, Noordwijk, The Netherlands, May 1992.

[5]Wingrove, R. C., "A Survey of Atmospheric Re-Entry Guidance and Control Methods, *AIAA Journal*, Vol. 1, No. 9, 1963, pp. 2019-2029.

[6]Duncan, R. C., "Guidance and Control for Atmospheric Entry," *Re-Entry and Planetary Entry Physics*, edited by W. H. Loh, Vol. II, Springer-Verlag, New York, 1968, pp. 205-256.

[7]Box, D. M., Harpold, J. C., Paddock, S. G., Armstrong, N. A., and Hamby, W. H., "Controlled Re-Entry," *Gemini Summary Conference*, NASA SP-138, Feb. 1967, pp. 159-166.

[8]Graves, C. A., and Harpold, J. C., "Apollo Experience Report—Mission Planning for Apollo Entry," NASA TN D-6725, March 1972.

[9]Harpold, J. C., and Graves, C. A., "Shuttle Entry Guidance," *Journal of the Astronautical Sciences*, Vol. 26, No. 3, 1979, pp. 239-268.

[10]Mease, K. D., and Kremer, J. P., "Shuttle Entry Guidance Revisited," AIAA Paper 92-4450-CP, Aug. 1992.

[11]Cramer, E. J., Bardt, J. E., and Hardtla, J. W., "NLP Re-Entry Guidance: Developing a Strategy for Low L/D Vehicles," *Journal of Guidance, Control, and Dynamics*, Vol. 14, No. 6, 1991, pp. 1181-1190; also AIAA Paper 88-4123-CP, 1988.

[12]Corban, J. E., Calise, A. J., and Flandro, G. A., "Rapid Near-Optimal Aerospace Plane Trajectory Generation and Guidance," AIAA Paper 91-2820-CP, 1991.

[13]Stiles, J. A., "Predictive Entry Guidance for an Apollo-Type Vehicle," *Proceedings of the 3rd IFAC Symposium on Automatic Control in Space* (Toulouse, France), International Federation of Automatic Control, Laxenburg, Austria, March 1970, pp. 732-740.

[14]Skaslecki, L., and Martin, M., "General Adaptive Guidance Using Nonlinear Programming Constraint Solving Methods (FAST)," AIAA Paper 91-2820-CP, 1991.

[15]Paus, M., "A General Approach to Optimal Real-Time Guidance of Dynamic Systems Based on Nonlinear Programming," *Proceedings of the AIAA Guidance, Navigation, and Control Conference* (Hilton Head, SC), AIAA, Washington, DC, Aug. 1992, pp. 297-305 (AIAA Paper 92-4378-CP).

[16]Beier, W., and Kallerhof, H., "Positionsbestimmung für Raumfahrzeuge mit dem Satellitennavigationssystem GPS [Space Vehicle Positioning with the Satellite Navigation System GPS]," *Elektrisches Nachrichtenwesen*, Vol. 62, No. 1, 1988, pp. 87-91.

[17]Jacob, T., and Dieroff, M., "Integrated Navigation for Approach Guidance Using Differential GPS," *Proceedings of the 1990 GPS Conference* (Colorado Springs, CO), American Inst. of Navigation, Washington, DC, Sept. 1990.

[18]Roenneke, A. J., and Cornwell, P. J., "Trajectory Control for a Low-Lift Maneuverable Re-Entry Vehicle," AIAA Paper 92-1146-CP, Feb. 1992.

[19]Roenneke, A. J., and Well, K. H., "Re-Entry Control of a Low-Lift Maneuverable Spacecraft," *Proceedings of the AIAA Guidance, Navigation, and Control Conference* (Hilton Head, SC), AIAA, Washington, DC, Aug. 1992, pp. 641-652 (AIAA Paper 92-4455-CP).

[20]Miele, A., *Flight Mechanics*, Addison-Wesley, Reading, MA, 1962.

[21]Vinh, N. X., *Optimal Trajectories in Atmospheric Flight*, Elsevier, New York, 1981.

[22]Battin, R. H., *Astronautical Guidance*, McGraw-Hill, New York, 1964.

[23]Bryson, A. E., and Ho, Y., *Applied Optimal Control*, Hemisphere Publishing, New York, 1975.

[24]Roenneke, A. J., *Trajectory Control for a Low-Lift Maneuverable Re-Entry Vehicle Using State Feedback*, M.S. Thesis, Rose-Hulman Inst. of Technology, Terre Haute, IN, May 1991.

[25]Anderson, B. D., and Moore, J. B., *Optimal Control*, Prentice-Hall, Englewood Cliffs, NJ, 1990.

[26]U.S. National Oceanic and Atmospheric Administration, *U.S. Standard Atmosphere 1976*, U.S. GPO, NOAA-S/T 76-1562, Washington, DC, 1976.

[27]Gamble, J. D., and Findlay, J. T., "Shuttle-Derived Densities in the Middle Atmosphere," AIAA Paper 88-4352-CP, 1988.

[28]Crowder, R. S., and Moote, J. D., "Apollo Entry Aerodynamics," *Journal of Spacecraft*, Vol. 6, March 1969, pp. 302-307.

[29]*Simulink—A Program for Simulating Dynamic Systems*, The MathWorks Inc., Natick, MA, 1992.